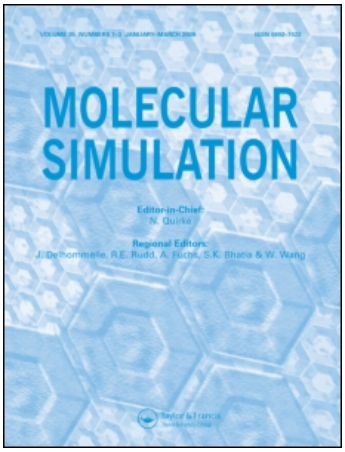

Molecular Simulation
Publication details, including instructions for authors and subscription information:
http://www.informaworld.com/smpp/title~content=t713644482

Brownian dynamics simulations of hydrophobic dendrimer adsorption

Balram Suman[a]; Satish Kumar[a]
[a] Department of Chemical Engineering and Materials Science, University of Minnesota, Minneapolis, MN, USA

First published on: 21 September 2010

To cite this Article Suman, Balram and Kumar, Satish(2009) 'Brownian dynamics simulations of hydrophobic dendrimer adsorption', Molecular Simulation, 35: 1, 38 — 49, First published on: 21 September 2010 (iFirst)
To link to this Article: DOI: 10.1080/08927020802191966
URL: http://dx.doi.org/10.1080/08927020802191966

Molecular Simulation
Vol. 35, Nos. 1–2, January–February 2009, 38–49

Taylor & Francis
Taylor & Francis Group

Brownian dynamics simulations of hydrophobic dendrimer adsorption

Balram Suman and Satish Kumar*

Department of Chemical Engineering and Materials Science, University of Minnesota, Minneapolis, MN, USA

(*Received 15 March 2008; final version received 9 May 2008*)

The adsorption of an isolated hydrophobic dendrimer onto a flat surface is studied in this work using Brownian dynamics simulations. The dendrimer is modelled as a freely jointed bead-rod chain. Bead–bead and bead–surface hydrophobic interactions along with excluded-volume interactions are accounted for using a Lennard-Jones potential. Adsorption behaviour is studied as a function of the strength of hydrophobic interactions, dendrimer generation and distribution of hydrophobic groups within the dendrimer. The adsorbed dendrimer adopts a disk-like conformation by compressing in the direction normal to the surface and expanding in the direction parallel to the surface. As the strength of hydrophobicity decreases, the adsorbed dendrimer expands in the normal direction and contracts in the parallel direction. Eventually, at a very low level of hydrophobicity, the dendrimer desorbs and adopts a sphere-like conformation. Bead density profiles show that the adsorbed hydrophobic dendrimer forms a two-layer structure, with one layer corresponding to adsorbed groups, and another layer in free solution, similar to charged dendrimer adsorption. However, unlike charged dendrimer adsorption, all terminal groups can be attached to a surface using a dendrimer having all hydrophobic groups or hydrophobic terminal groups. In the case of a dendrimer having only hydrophobic branching groups, most of the terminal groups can be placed in free solution. Also, an adsorbed hydrophobic dendrimer forms a relatively compact structure unlike the stretched configuration of adsorbed charged dendrimers. The results presented here suggest how to tune the levels of hydrophobicity and charge to tailor dendrimer surface conformations, and may help guide hydrophobic dendrimer design for applications such as drug delivery and surface functionalisation.

Keywords: dendrimer; adsoprtion; hydrophobic; Brownian dynamics

1. Introduction

Dendrimers are nearly monodisperse polymers with a highly branched three-dimensional structure. They can easily move across biological membranes after customising and controlling dendrimer architecture, and can store a wide range of metals, organic or inorganic molecules and genetic materials among their branches. These characteristics make them suitable for applications involving drug delivery, membranes, adhesion, microelectronics and chemical and biological sensors [1–6]. One important class of dendrimers is that in which hydrophobic groups are present. The distribution of hydrophobic groups within dendrimers can be altered for various applications [6–10]. For example, a dendrimer having a hydrophobic interior and a hydrophilic exterior can be used to form complexes with hydrophobic drugs, resulting in water-soluble drugs [11]. Thus, in view of the drug delivery applications of hydrophobic dendrimers, it is important to investigate adsorption of hydrophobic dendrimers. In particular, it is important to consider various distributions of hydrophobic groups within a dendrimer since dendrimer–surface interactions will govern dendrimer adsorption and conformations. In this work, we apply Brownian dynamics (BD) simulations to investigate the behaviour of an isolated hydrophobic dendrimer near surfaces.

Theoretical and experimental studies of charged and neutral dendrimers in free solution are well documented in Ballauff and Likos [12] and references therein. Experimental investigations of charged dendrimer adsorption have also been presented [13–21]. These studies report that adsorption of charged dendrimers is due to dendrimer–surface electrostatic interactions and that the adsorbed dendrimers resemble flat disks. The amount of adsorbed dendrimer can be increased by increasing dendrimer generation [17,18] and surface charge density [17,20,21], and can be decreased by increasing salt concentration [17]. Kleijn et al. [15] mentioned that along with electrostatic interactions, non-electrostatic interactions also play an important role in dendrimer adsorption. Suman and Kumar [22] performed BD simulations of isolated charged dendrimer adsorption and employed Debye-Hückel potentials for electrostatic interactions. They found that adsorbed dendrimers adopt a flat disk-like structure and that terminal groups can be distributed at the dendrimer periphery or placed within the adsorbed dendrimer volume depending on the dendrimer charge distribution.

Theoretical investigations of dendrimer adsorption involving non-electrostatic dendrimer–surface interactions have also been presented [19,23–25]. Mansfield [23] performed simulations for dendrimer adsorption

*Corresponding author. Email: kumar@cems.umn.edu

ISSN 0892-7022 print/ISSN 1029-0435 online

DOI: 10.1080/08927020802191966
http://www.informaworld.com

where only odd branching points (first, third, fifth, etc.) are attracted to a surface. He mentioned that although there is no good reason to use this particular surface interaction, it still possesses many interesting properties that are expected of real dendrimers adsorbing onto a surface. He found that an adsorbed dendrimer is compressed in the direction normal to and extended in the direction parallel to the adsorbing surface. Also, the minimum strength of dendrimer–surface interactions for dendrimer adsorption decreases as dendrimer generation increases. Striolo and Prausnitz [24] investigated dendrimer adsorption using dendrimer–surface interactions in the form of square-well potentials. The dendrimers were modelled as freely jointed hard spheres with all spheres being attracted to the surface. They found that dendrimers are easier to adsorb than linear polymers since dendrimers pay a lower entropic penalty upon adsorption due to their globular structures. Mecke et al. [19] studied the adsorption of neutral dendrimers using atomic force microscopy experiments. They also performed atomistic molecular dynamics simulations of terminally charged and neutral poly(amidoamine) (PAMAM) dendrimers near a mica surface. They reported that the adsorbed dendrimer thickness and its extension parallel to the surface are not significantly changed by replacing a charged dendrimer with a neutral one. Ratner et al. [25] performed BD simulations of a third-generation dendrimer adsorbing onto an attractive surface by employing a freely jointed bead-rod model for the dendrimer and using a Lennard-Jones potential for excluded-volume and dendrimer–surface interactions. They observed that as the strength of the attraction increases, the dendrimer–surface contact area increases.

In the case of hydrophobic dendrimer adsorption, two hydrophobic dendrimer groups attract each other unlike the repulsion between dendrimer groups in the charged dendrimer case [22]. In the studies by Mansfield [23] and Striolo and Prausnitz [24], there were no interactions between dendrimer groups. In this study, we employ a Lennard-Jones potential to account for hydrophobic and excluded-volume interactions between dendrimer groups and between dendrimer groups and surfaces. The strength of hydrophobicity has been accounted for using a parameter in the Lennard-Jones potential similar to that used in previous studies [26–28] for modelling hydrophobic interactions between two spheres. Apart from the work of Ratner et al. [25], we are not aware of any study which uses a Lennard-Jones potential for dendrimer–surface interactions. We note that Ratner et al. [25] confined their study only to a third-generation dendrimer where all dendrimer groups are attracted to the surface.

In this work, we extend the study of [22] by investigating adsorbed hydrophobic dendrimer behaviour as a function of the strength of hydrophobicity, distribution of hydrophobic groups within the dendrimer and dendrimer generation. Three different hydrophobic group distributions are considered: (i) all hydrophobic groups, (ii) only hydrophobic terminal groups and (iii) only hydrophobic branching groups. In addition, the effects of electrostatic interactions along with the hydrophobic interactions have also been investigated. The rest of the paper is organised as follows: the simulation model and algorithm are discussed in Section 2, results and a discussion are presented in Section 3, and a summary and conclusions are given in Section 4.

2. Simulation model and algorithm

We model a dendrimer molecule as a freely jointed bead-rod chain. Each bead of the model dendrimer represents a monomer, and a frictional drag acts on it with a friction coefficient ζ. The length of a rod, l, connecting two beads is the distance between two adjacent connected monomers. We consider a trifunctional monomer, and thus three beads are connected to every branching bead using a rod between them. Such a coarse-grained model has previously been employed to study dendrimer behaviour in free solution, and simulation results are in agreement with experimental observations [29–31]. The number of branching beads encountered between the dendrimer core and a peripheral bead is called the dendrimer generation, G. The number of beads, N, in a dendrimer having trifunctional monomers is:

$$N = 3(2^{G+1} - 1) + 1. \tag{2.1}$$

In this work, we consider excluded-volume and hydrophobic interactions. In some cases, the effects of electrostatic interactions are also accounted for. Electrostatic interactions similar to the ones used in Suman and Kumar [22] have been employed.

Oss et al. [32] reported that the preferential attraction due to hydrophobic effects can be described using van der Waals interactions, and a number of researchers employed a 6–12 Lennard-Jones potential to model hydrophobic and excluded-volume effects [26–28]. In this work, these interactions between the ith and the jth beads are described by:

$$U^{\mathrm{LJ}}(r_{ij}) = 4\varepsilon\left[\left(\frac{\sigma}{r_{ij}}\right)^{12} - m\left(\frac{\sigma}{r_{ij}}\right)^{6}\right], \tag{2.2}$$

where r_{ij} is the distance between the ith and the jth beads, and m is 1 if the ith and the jth beads are hydrophobic; otherwise it is zero [27]. We have employed the parameters $\sigma = 0.8l$ and $\varepsilon = 0.3k_{\mathrm{B}}T$, with $k_{\mathrm{B}}T$ being the product of Boltzmann's constant and temperature. These were used by Rey et al. [33] to reproduce the mean-square end-to-end length of a linear chain in a theta-solution. Since then, these parameters values have been used in several dendrimer simulation studies [29–31]. Recently, Ratner et al. [25] employed these parameters for their

investigation of dendrimer adsorption. In their studies, $m = 1$ is used for all i and j combinations. However, in this study, we consider dendrimers having different hydrophobic group distributions, and $m = 1$ only when both i and j correspond to hydrophobic beads. The force due to the Lennard-Jones interactions is:

$$\mathbf{F}_{ij}^{\mathrm{LJ}} = \begin{cases} 24\varepsilon\left[2\left(\frac{\sigma}{r_{ij}}\right)^{12} - m\left(\frac{\sigma}{r_{ij}}\right)^{6}\right]\frac{\hat{\mathbf{r}}_{ij}}{r_{ij}}, & r_{ij} < 2.5\sigma \\ 0, & r_{ij} \geq 2.5\sigma \end{cases}, \quad (2.3)$$

where $\hat{\mathbf{r}}_{ij}$ is the unit vector along r_{ij}, and the cutoff radius is 2.5σ [31]. The total force acting on bead i is the sum of the forces due to all other beads, i.e. $\mathbf{F}_i^{\mathrm{LJ}} = \sum_{i \neq j} \mathbf{F}_{ij}^{\mathrm{LJ}}$.

The force between a bead and a surface is obtained after integrating the Lennard-Jones potential over the surface. Such an integration of the Lennard-Jones potential has also been performed when investigating the static and dynamic properties of polymer melts confined between two planar surfaces [34]. The bead–surface potential energy associated with the ith bead is:

$$V_i^H = 2\pi A\left[\frac{2}{5}\left(\frac{\sigma_w}{z_i}\right)^{10} - m\left(\frac{\sigma_w}{z_i}\right)^{4}\right], \quad (2.4)$$

where A is the parameter representing the strength of the hydrophobic attraction and z_i is the distance of the ith bead above the surface, which is located at $z = 0$. Here, $m = 1$ if the ith bead is hydrophobic (otherwise $m = 0$), and σ_w is a length scale for the hydrophobic interactions. If the distance between the surface and the dendrimer is higher than σ_w the attractive component (second-term of Equation (2.4)) of V_i^H dominates; otherwise the repulsive component (first-term of Equation (2.4)) dominates. The force on the ith bead due to the surface is given as:

$$\mathbf{F}_i^H = \begin{cases} 8\pi\frac{A}{\sigma_w}\left[\left(\frac{\sigma_w}{z_i}\right)^{11} - m\left(\frac{\sigma_w}{z_i}\right)^{5}\right]\hat{\mathbf{k}}, & z_i \geq 0.8l \\ 8\pi\frac{A}{\sigma_w}\left[\left(\frac{\sigma_w}{z_c}\right)^{11} - m\left(\frac{\sigma_w}{z_c}\right)^{5}\right]\hat{\mathbf{k}}, & z_i \leq 0.8l \end{cases}, \quad (2.5)$$

where $\hat{\mathbf{k}}$ is the unit vector in the z-direction. In our simulations, we have taken $\sigma_w = 1$ and $z_c = 0.8l$. For computational ease, the repulsive force is taken to be constant for $z_i \leq 0.8l$, and the constant force is evaluated at $z_i = 0.8l$.

Similar to Suman and Kumar [22], bead–bead electrostatic interactions are modelled using a screened Coulombic (Debye-Hückel) potential. The bead–bead electrostatic repulsion force on bead i is:

$$\mathbf{F}_i^R = \sum_{i \neq j} k_{\mathrm{B}} T l_{\mathrm{B}} q^2 \left(\frac{1}{r_{ij}} + \kappa\right)\frac{e^{-\kappa r_{ij}}}{r_{ij}}\hat{\mathbf{r}}_{ij}, \quad (2.6)$$

where q is the non-dimensional charge on each charged bead (made dimensionless by the electronic charge, e), $l_{\mathrm{B}} = e^2/(4\pi\varepsilon k_{\mathrm{B}}T)$ is the Bjerrum length for a medium of permittivity ε, and κ is the inverse screening length, representing the strength of screening. In the case of a binary electrolyte, $\kappa^2 = 8\pi z^2 l_{\mathrm{B}} c$, where z is the valence of a salt ion and c is the salt concentration. Higher κ corresponds to higher salt concentration.

The electrostatic force acting on a charged bead due to a uniformly charged surface of opposite sign is given by the product of bead charge and the electric field due to the surface. Similar to Suman and Kumar [22], the force on the ith bead due to the surface is:

$$\mathbf{F}_i^E = -4\pi k_{\mathrm{B}} T \sigma_{\mathrm{s}} \frac{l_{\mathrm{B}}}{l^2}\hat{\mathbf{k}}. \quad (2.7)$$

The quantity σ_{s} is the non-dimensional magnitude of the surface charge density (made dimensionless by e/l^2).

The Ermak–McCammon algorithm [35] is used to obtain bead positions where each integration step is calculated according to:

$$\mathbf{r}_i = \mathbf{r}_i^o + (\Delta t/(k_{\mathrm{B}}T))\sum_j \mathbf{D}_{ij}^o \cdot \mathbf{F}_j^o + \mathbf{\Phi}_i^o, \quad (2.8)$$

where the superscript 'o' indicates the variables to be evaluated at the beginning of the time-step, and thus $\mathbf{r}_i^o$ and $\mathbf{r}_i$ represent the position vectors for the ith bead before and after the time-step. The time-step size is denoted by Δt, and $\mathbf{D}_{ij}^o$ is the diffusion tensor with all diagonal elements $k_{\mathrm{B}}T/\zeta$. The term $\mathbf{\Phi}_i^o$ is a random (Gaussian) displacement with zero mean and variance $2\mathbf{D}_{ij}^o\Delta t$. The quantity $\mathbf{F}_j^o$ is the sum of all the forces acting on the jth bead:

$$\mathbf{F}_j^o = \mathbf{F}_j^{\mathrm{LJ}} + \mathbf{F}_j^R + \mathbf{F}_j^E + \mathbf{F}_j^H. \quad (2.9)$$

As rod lengths have to remain constant, the SHAKE algorithm [36,37] is employed to maintain constant rod lengths with a tolerance of $2 \times 10^{-6} l$. A discussion of this algorithm can be found in Ref. [22]. For non-dimensionalisation, we have used l for length, $k_{\mathrm{B}}T$ for energy and $\zeta l^2/k_{\mathrm{B}}T$ for time. Henceforth, all variables are taken to be dimensionless and the same variables have been used to denote them. In our simulations, we have varied A, and when electrostatic interactions have been considered, we have used $q = 1$, $\sigma_{\mathrm{s}} = 2$ and $l_{\mathrm{B}} = 1$. The values of A and the electrostatic parameters we consider are consistent with what can be achieved experimentally [14,19,23,25,26,32,38–43]. The time-step is chosen so that the maximum bead displacement in a single step does not exceed 10% of the rod length. For most of the simulations, a time-step of $\Delta t = 5 \times 10^{-5}$ is used. Initial dendrimer configurations are generated with a procedure proposed by Murat and Grest [44], and values of G up to 5 have been probed.

To start a simulation, the core bead is placed at a distance $d = 3$ from the surface in order to prevent beads from crossing the surface. After a suitable initial configuration is generated, bead positions are evolved with time. We calculate the time-averaged values of various conformational properties obtained after the dendrimer reaches steady state. The total number of integration steps is typically $\sim 5 \times 10^7$, which is much longer (>50 times) than the time it takes to reach steady state. The results presented here do not change substantially for smaller time-step sizes, longer integration times, or smaller values of d. Our simulations of hydrophobic dendrimer adsorption capture the adsorption behaviour presented in Ratner et al. [25], i.e. an increase in the dendrimer–surface contact area as the parameter in the Lennard-Jones potential representing the strength of the dendrimer–surface attraction increases.

3. Results and discussion

3.1 Hydrophobic dendrimer near surface

3.1.1. Dendrimer conformation

Dendrimer conformations are characterised in terms of the radius of gyration, R_g, and its components in the parallel (planar; x- and y-), $R_{g\|}$, and perpendicular (z-), R_{gz}, directions:

$$R_g = \sqrt{\frac{\left\langle \sum_{i=1}^{N} [(x_i - x_{cm})^2 + (y_i - y_{cm})^2 + (z_i - z_{cm})^2] \right\rangle}{N}},$$

$$R_{g\|} = \sqrt{\frac{\left\langle \sum_{i=1}^{N} [(x_i - x_{cm})^2 + (y_i - y_{cm})^2] \right\rangle}{N}},$$

$$R_{gz} = \sqrt{\frac{\left\langle \sum_{i=1}^{N} (z_i - z_{cm})^2 \right\rangle}{N}}, \tag{3.1}$$

where (x_i, y_i, z_i) is the position of the ith bead, (x_{cm}, y_{cm}, z_{cm}) is the centre-of-mass of the dendrimer, and the broken brackets denote a time average. Figure 1 presents the variation of R_g and its components with A for dendrimers having different hydrophobic group distributions. For a dendrimer having hydrophobic terminal beads, R_g is nearly constant as A increases, and R_g increases as G increases (Figure 1(a)). A similar variation of R_g with A in the work of Mansfield [23] was found where alternate branching beads were attracted to a surface. However, with a dendrimer having all hydrophobic or hydrophobic branching beads, R_g first increases as we increase A, then decreases, and eventually becomes nearly constant. The nature of the variation of R_g with A will be discussed after presenting $R_{g\|}$ and R_{gz}.

For a dendrimer having hydrophobic terminal groups, $R_{g\|}$ first increases and eventually becomes nearly constant as A increases (Figure 1(b)). At low A, the dendrimer is in free solution with a spherical three-dimensional structure, and as A increases, it comes near the attractive surface. The adsorbed dendrimer adopts a nearly two-dimensional

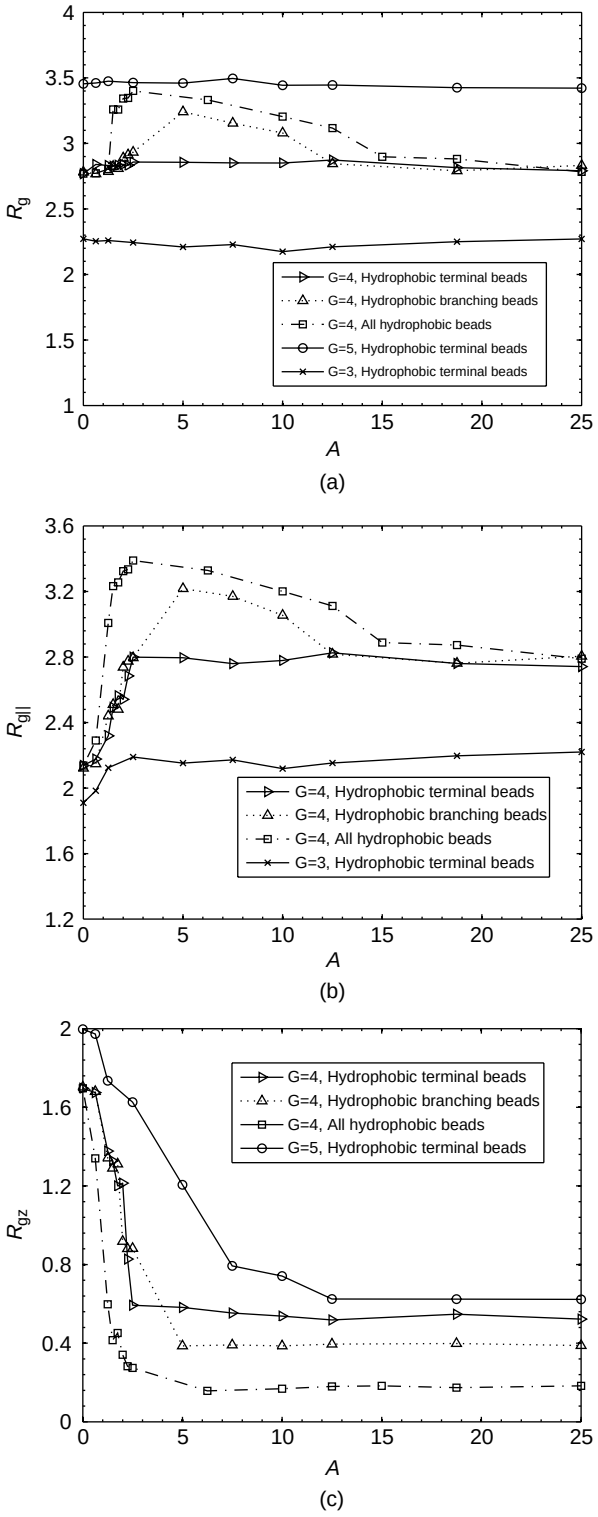

Figure 1. Plots of R_g and its components versus A of a hydrophobic dendrimer having various hydrophobic group distributions: (a) R_g, (b) $R_{g\|}$ and (c) R_{gz}.

structure, resulting in higher $R_{g\|}$. In contrast, we find a pronounced peak in $R_{g\|}$ for a dendrimer having all hydrophobic or hydrophobic branching groups. The reason for the increase in $R_{g\|}$ with A at low A is the same as that for a dendrimer having hydrophobic terminal groups. However, the reduction in $R_{g\|}$ as A further increases is due to the bead–bead attraction among branching beads: a larger number of branching beads are near the surface as A increases, placing these beads close to each other. This enhances the bead–bead attraction and leads to a reduction in $R_{g\|}$ with increasing A at high A. To validate this explanation, we have performed simulations for dendrimers having these two hydrophobic group distributions but without bead–bead attraction, and we do not find the reduction in $R_{g\|}$ with increasing A. With hydrophobic dendrimers at higher A, $R_{g\|}$ remains nearly constant as A increases since the attractive bead–bead potential is balanced by the repulsive excluded-volume potential.

For hydrophobic dendrimers, R_{gz} decreases as A increases (Figure 1(c)), and R_{gz} is largest for an adsorbed dendrimer having hydrophobic terminal groups. This is followed by an adsorbed dendrimer having hydrophobic branching groups, and R_{gz} is the smallest for an adsorbed dendrimer having all hydrophobic groups. For the dendrimer having all hydrophobic groups, the adsorbed dendrimer spreads as nearly a monolayer of beads onto the surface, resulting in smaller R_{gz}. In the case of a dendrimer having hydrophobic terminal or branching groups, only terminal or only branching beads are attached to the surface, respectively, resulting in higher R_{gz}.

The behaviour of R_g can be understood from the behaviour of $R_{g\|}$ and R_{gz}. For the case of a dendrimer having hydrophobic terminal groups, an increase in $R_{g\|}$ is compensated by a reduction in R_{gz} with increasing A, resulting in nearly constant R_g. However, with dendrimers having the other two hydrophobic group distributions, the variation in R_g with A is governed by $R_{g\|}$ due to a pronounced peak in $R_{g\|}$, resulting in a non-monotonic variation of R_g with A.

The minimum strength of hydrophobic interactions required for dendrimer adsorption is a quantity of interest. A dendrimer is considered adsorbed if its centre-of-mass in the direction normal to the surface (z_{cm}) fluctuates by less than 10%. The critical A for fourth-generation dendrimers having all hydrophobic groups is $\sim$1, for dendrimers having hydrophobic terminal groups, it is $\sim$1.2, and for dendrimers having hydrophobic branching groups, it is $\sim$1.4. The critical A for the dendrimer having all hydrophobic groups is lower due to a larger number of hydrophobic beads. The number of hydrophobic beads is nearly equal for dendrimers having the other two hydrophobic group distributions. However, the critical A is higher for a dendrimer having hydrophobic branching groups due to steric hindrance. The critical A increases as G decreases [23] since a smaller dendrimer pays a higher entropic penalty for adsorption [24].

It is important to compare the behaviour of R_g and its components found in this work with that of an adsorbed charged dendrimer [22]. In the case of an adsorbed charged dendrimer, bead–bead repulsion acts among charged beads, whereas bead–bead attraction is present in the case of an adsorbed hydrophobic dendrimer. In addition, the expressions for bead–surface interactions in these two cases are different (cf. Equations (2.5) and (2.7)). In the case of an adsorbed charged dendrimer, R_g monotonically increases as the dendrimer–surface electrostatic attraction increases. This occurs since bead–bead electrostatic repulsion increases as dendrimer–surface electrostatic attraction increases. In contrast, for a dendrimer having hydrophobic terminal groups, R_g is nearly constant with an increase in the strength of dendrimer–surface hydrophobic interactions. For dendrimers having the other two hydrophobic group distributions, R_g has a pronounced peak, and eventually R_g of an adsorbed dendrimer at high A is nearly the same as that in free solution.

The parallel component of R_g of an adsorbed charged dendrimer also monotonically increases as the dendrimer–surface electrostatic attraction increases. Since an adsorbed dendrimer adopts a flat disk-like structure and increasing the dendrimer–surface electrostatic attraction increases bead–bead repulsion, this expands the adsorbed dendrimer in the direction parallel to the surface ($R_{g\|}$ increases). However, for a dendrimer having hydrophobic terminal groups, $R_{g\|}$ first increases and then becomes nearly constant as A increases. For dendrimers having the other two hydrophobic group distributions, $R_{g\|}$ has a pronounced peak, and eventually $R_{g\|}$ is nearly constant with increasing A, and is higher than $R_{g\|}$ of a respective dendrimer in free solution.

For an adsorbed charged dendrimer, R_{gz} decreases as the strength of the dendrimer–surface electrostatic attraction increases. Similarly, in the case of hydrophobic dendrimer adsorption, R_{gz} first decreases and then becomes nearly constant with increasing A at high A, where the dendrimer–surface hydrophobic attraction becomes comparable to the excluded-volume interaction. Similar to charged dendrimer adsorption, the nature of the variation of R_g and its components does not change with G for adsorbed hydrophobic dendrimers.

3.1.2. *Monomer distribution within dendrimer*

In the previous section, we have discussed adsorbed hydrophobic dendrimer conformations. It is also important to know where monomers and terminal groups are within the dendrimer. Thus, we now present monomer and terminal group distributions within a dendrimer using total and terminal bead densities as a function of the distance

from the dendrimer centre-of-mass (r). These densities have been obtained in a manner similar to that presented in Suman and Kumar [22].

We first consider how monomer and terminal group distributions change with the strength of dendrimer–surface hydrophobic interactions. In Figure 2, we present the total and terminal bead densities as a function of r for a dendrimer having hydrophobic terminal groups. At low A ($A = 0$ and 0.625), where dendrimers are in free solution, the total bead density has a maximum at the centre-of-mass (Figure 2(a)). However, at high A where dendrimers are adsorbed, we find a more pronounced peak in the density profile slightly away from the centre-of-mass. For an adsorbed dendrimer, the terminal beads come close together and the attraction between them keeps them slightly away from the centre-of-mass. This is further illustrated in Figure 2(b) where we find a pronounced peak in the terminal density profile for high A at nearly the same place where there is a peak in the total density profile. From Figure 2(b), we also find that terminal beads come closer to the centre-of-mass as A increases.

We present in Figure 3 the effects of hydrophobic group distributions on monomer and terminal bead density for adsorbed hydrophobic dendrimers. We find that the maxima and minima in the total bead density profile are pronounced for a dendrimer having all hydrophobic groups or hydrophobic branching groups (Figure 3(a)). This is due to a larger number of beads being attached to the surface, resulting in branching beads being close to each other, which enhances the bead–bead attraction among branching beads. Thus, some of the beads are lying on concentric circles and we find pronounced maxima and minima in the total bead density profile. For the dendrimer having all hydrophobic groups, the maximum is at the centre-of-mass due to attraction to the core bead. As attraction between terminal beads and interior beads is absent for a dendrimer having hydrophobic terminal groups, beads are more uniformly distributed in the

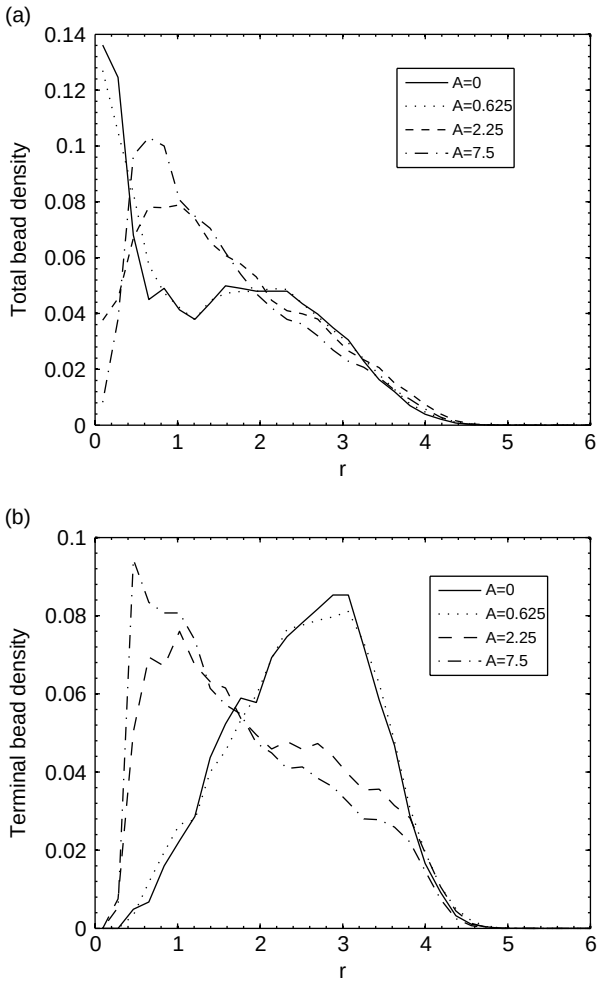

Figure 2. Total bead density and terminal bead density versus the distance from dendrimer centre-of-mass for a $G = 4$ dendrimer having hydrophobic terminal groups: (a) total bead density and (b) terminal bead density.

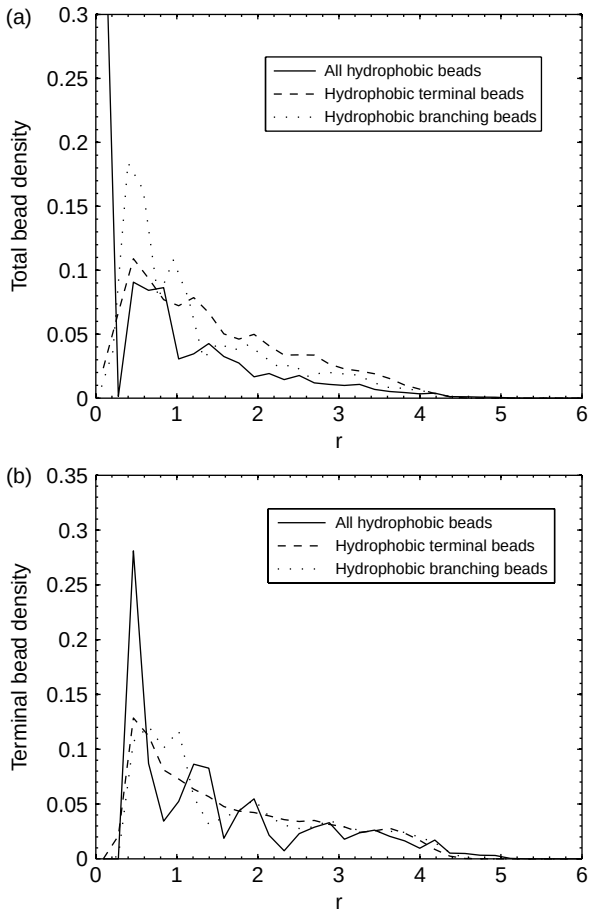

Figure 3. Total bead density and terminal bead density versus the distance from dendrimer centre-of-mass for a $G = 4$ hydrophobic dendrimer with $A = 12.5$: (a) total bead density and (b) terminal bead density.

dendrimer volume (Figure 3(a)). Again, due to the bead–bead attraction, the terminal bead density profile for the dendrimer having all hydrophobic groups also has pronounced maxima and minima (Figure 3(b)). Suppressed maxima and minima in the terminal bead density profile for a dendrimer having hydrophobic branching groups are present since along with branching beads, some of the terminal beads are also lying on concentric circles. In the case of the adsorbed dendrimer having hydrophobic terminal groups, terminal beads are distributed more uniformly throughout the dendrimer.

Varying dendrimer generation does not change the nature of the total and terminal bead density profiles. However, the total and terminal bead densities increase with an increase in G since the increase in the number of beads (cf. Equation (2.1)) is higher than that in dendrimer volume as G increases [22].

We again compare the total and terminal bead densities for an adsorbed hydrophobic dendrimer with those for an adsorbed charged dendrimer [22]. With charged dendrimer adsorption, the maxima and minima of the total bead density profile become more pronounced as the strength of dendrimer–surface attraction increases. This is due to the stretching of dendrons as a result of bead–bead repulsion, which places beads of an adsorbed charged dendrimer on concentric circles with their centres at the core bead. In contrast, with an adsorbed dendrimer having hydrophobic terminal groups, we obtain only one pronounced peak slightly away from the centre-of-mass, and the peak becomes more and more pronounced as A increases. However, with dendrimers having the other two hydrophobic group distributions, we obtain maxima and minima in the profile. But, these peaks are much suppressed compared to those for adsorbed charged dendrimers. With a dendrimer having charged terminal groups or all charged groups, terminal beads are at the dendrimer periphery due to bead–bead repulsion. With an adsorbed dendrimer having charged branching groups, terminal beads are distributed in its volume, but away from the centre-of-mass. In contrast, we find that terminal beads are slightly away from the centre-of-mass for adsorbed dendrimers having all three hydrophobic group distributions. Similar to adsorption of charged dendrimers, the nature of these density profiles does not vary with G for adsorbed hydrophobic dendrimers.

3.1.3. Monomer distribution near surface

It is important to investigate where monomers and terminal groups are with respect to the attractive surface. We obtain the distribution of monomers and terminal groups as a function of the distance from the surface (d) in terms of total and terminal bead densities. These densities have been obtained in a manner similar to that used in Suman and Kumar [22].

We first investigate the effects of dendrimer–surface interactions on monomer and terminal group distributions near the surface. In Figure 4, we present the total bead density and terminal bead density profiles as a function of the distance from the hydrophobic surface for a dendrimer having hydrophobic terminal groups. The peak near the surface gives a measure of the number of beads attached to the surface. We find that most of the beads are attached to the surface. However, some of the beads remain in free solution at all A (Figure 4(a)). As A increases, the number of beads attached to the surface increases, scaling as $A^{0.8}$ at low A, and $A^{0.2}$ at high A. At very high A, the number of beads attached to the surface does not vary with A. We find that nearly all terminal beads are localised near the surface for an adsorbed dendrimer having hydrophobic terminal beads (Figure 4(b)); beads are considered attached to the surface if they are within $1.5l$ from the surface. The distance over which terminal beads are distributed decreases as A increases.

We next investigate the effects of hydrophobic group distributions on monomer and terminal group distributions

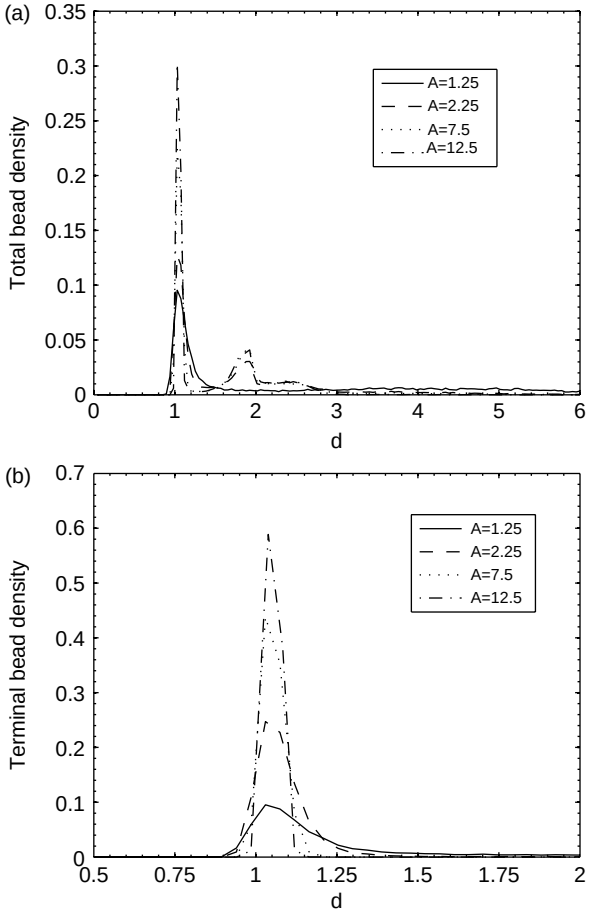

Figure 4. Total bead density and terminal bead density with respect to the distance from the surface for a $G = 4$ dendrimer having hydrophobic terminal groups: (a) total bead density and (b) terminal bead density.

near the surface. We present the total bead density and terminal bead density profiles for dendrimers having various hydrophobic group distributions in Figure 5. As the peak near the surface gives a measure of the number of beads attached to the surface, and that far from the surface gives the measure of the number of beads in free solution, the number of beads attached to the surface is maximum and that in free solution is minimum for a dendrimer having all hydrophobic groups (Figure 5(a)) since a dendrimer with this hydrophobic group distribution has largest number of hydrophobic beads. The number of beads attached to the surface for dendrimers having either hydrophobic terminal groups or hydrophobic branching groups is nearly the same (Figure 5(a)) since the number of hydrophobic beads for these two distributions is nearly the same. Considering the terminal bead density profiles in Figure 5(b), with a dendrimer having all hydrophobic groups or hydrophobic terminal groups, nearly all terminal beads are attached to the surface. However, with a dendrimer having hydrophobic branching groups, only some of the terminal beads are attached to the surface while others remain in free solution.

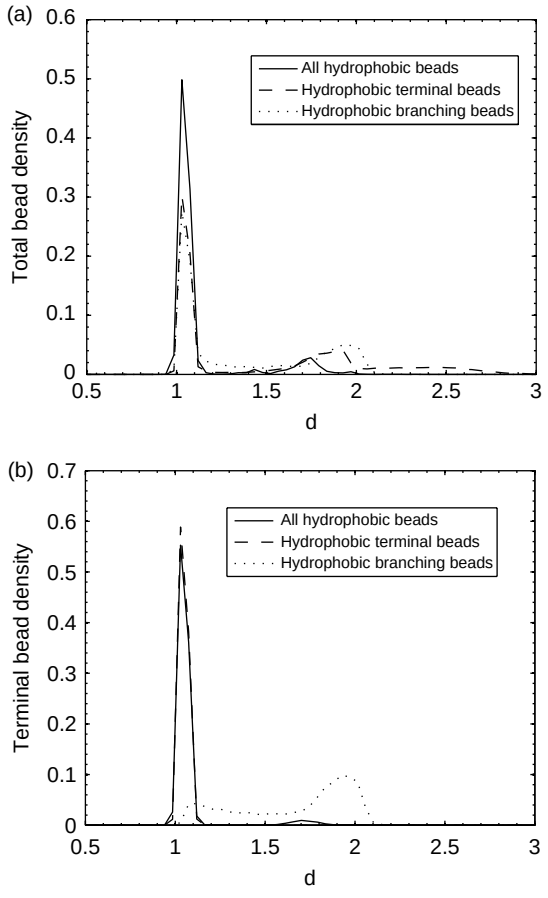

Figure 5. Total bead density and terminal bead density with respect to the distance from the surface for a $G = 4$ hydrophobic dendrimer: (a) total bead density and (b) terminal bead density.

As we increase dendrimer generation, the number of beads attached to the surface increases. Again, this is due to an exponential-like increase in the number of beads of a dendrimer with generation (cf. Equation (2.1)), which is higher than the increase in the contact area between the dendrimer and the surface. However, the nature of the total and terminal bead density profiles remains the same. The number of adsorbed beads for a dendrimer having hydrophobic terminal beads scales as $\sim G^{2.5}$, which shows that a larger number of beads can be attached to the surface compared to a terminally charged dendrimer where the scaling is $\sim G^{1.2}$ at low G and $\sim G^{0.3}$ at higher G [22]. Since with a hydrophobic dendrimer, the bead–bead electrostatic repulsion is absent and instead the bead–bead hydrophobic attraction acts among hydrophobic beads, a larger number of beads come near the surface.

We next compare the total and terminal bead densities near the surface for an adsorbed hydrophobic dendrimer with those for an adsorbed charged dendrimer [22]. Similar to an adsorbed charged dendrimer, as the strength of dendrimer–surface interactions increases, the number of beads near the surface also increases for an adsorbed hydrophobic dendrimer, and we also find two peaks in the total density profiles. The peak close to the surface corresponds to adsorbed beads and that far from the surface corresponds to the beads in free solution. For a dendrimer having all charged beads or charged terminal beads, the terminal bead density profile shows that most of the terminal beads are attached to the surface, but some of the terminal beads are in free solution. In contrast, with a dendrimer having all hydrophobic beads or hydrophobic terminal beads, nearly all terminal beads are attached to the surface due to the absence of bead–bead electrostatic repulsion and also the presence of bead–bead hydrophobic attraction. The total and terminal bead density profiles for a dendrimer having charged branching beads are similar to those for a dendrimer having hydrophobic branching beads. Similar to charged dendrimer adsorption, the nature of these density profiles does not change with G for adsorbed hydrophobic dendrimers.

3.2 Hydrophobic and charged dendrimer near surface

Adsorption behaviour of an isolated charged dendrimer is studied in Suman and Kumar [22], and that of an isolated hydrophobic dendrimer is investigated in the previous sections. In this section, we study adsorption of a dendrimer having both hydrophobicity and charge onto an oppositely charged surface. This will provide insight into how these two interactions compete with each other since, as discussed in the previous sections, adsorbed hydrophobic dendrimers have different conformations near surfaces than adsorbed charged dendrimers. Furthermore, this could also yield unique dendrimer structures

near surfaces, which could not be obtained without applying charge and hydrophobic interactions together.

3.2.1. Dendrimer conformation

We first investigate the effects of bead–bead and dendrimer–surface electrostatic and hydrophobic interactions on R_g and its components for a dendrimer having charged and hydrophobic terminal groups. In Figure 6, we present R_g and its components as a function of A for various κ. We find that at low κ, R_g first decreases and eventually remains nearly constant as A increases (Figure 6(a)). At low κ and low A, R_g is larger since the bead–bead electrostatic repulsion is stronger and bead–bead hydrophobic interaction is weaker as beads are far apart. As A increases, the bead–bead hydrophobic attraction increases since beads come close to each other, causing R_g to decrease. At high A, the bead–bead hydrophobic attraction dominates the bead–bead electrostatic repulsion, resulting in nearly constant R_g with A, similar to a neutral hydrophobic dendrimer (cf. Figure 1). As κ increases, the bead–bead electrostatic repulsion decreases, thus the bead–bead hydrophobic attraction dominates the bead–bead electrostatic repulsion even at lower A, resulting in a weakening of the behaviour where R_g decreases as A increases. Also, as κ increases, R_g decreases at all A. At high κ, the bead–bead electrostatic repulsion is very weak, and the nature of R_g is determined by the bead–bead hydrophobic interactions. Then, the variation in R_g is like that of a neutral hydrophobic dendrimer (cf. Figure 1).

The behaviour of $R_{g\|}$ and R_{gz} can also be explained in a similar way. At low κ and low A, the bead–bead electrostatic repulsion governs the nature of $R_{g\|}$ and R_{gz}; otherwise, bead–bead hydrophobic attraction governs their nature. For example, at low κ, $R_{g\|}$ decreases, and at high A, $R_{g\|}$ is nearly constant as A increases (Figure 6(b)). As both electrostatic and hydrophobic interactions increase, R_{gz} decreases (Figure 6(c)).

3.2.2. Monomer distribution

We have seen in the last section that the variation of R_g and its components with κ and A can be explained by separately considering electrostatic and hydrophobic interactions. Thus, instead of presenting various density profiles, we present the distinguishing features of an adsorbed charged dendrimer, an adsorbed hydrophobic dendrimer and an adsorbed charged and hydrophobic dendrimer using snapshots of typical conformations near surfaces. Snapshots presented in Figure 7(a),(d),(g) are for charged dendrimers, those in Figure 7(b),(e),(h) are for hydrophobic dendrimers, and Figure 7(c),(f),(i) are for charged and hydrophobic dendrimers. To show distinguishing features of adsorbed dendrimers, snapshots

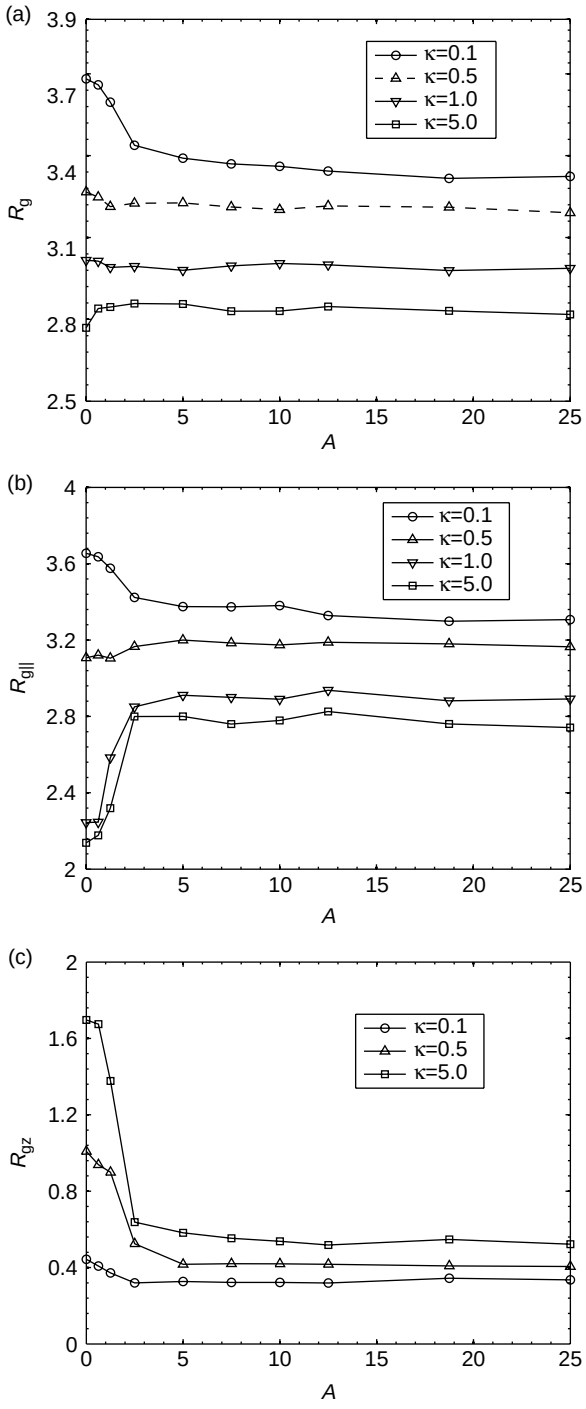

Figure 6. Plot of R_g and its components versus A for a dendrimer having charged and hydrophobic terminal groups: (a) R_g, (b) $R_{g\|}$ and (c) R_{gz}.

from different angles have been presented for each type of dendrimer. Also, to show an adsorbed charged and hydrophobic dendrimer conformation, we employ a different hydrophobicity strength.

We first discuss an adsorbed charged dendrimer and an adsorbed hydrophobic dendrimer. Comparing Figure 7(a)

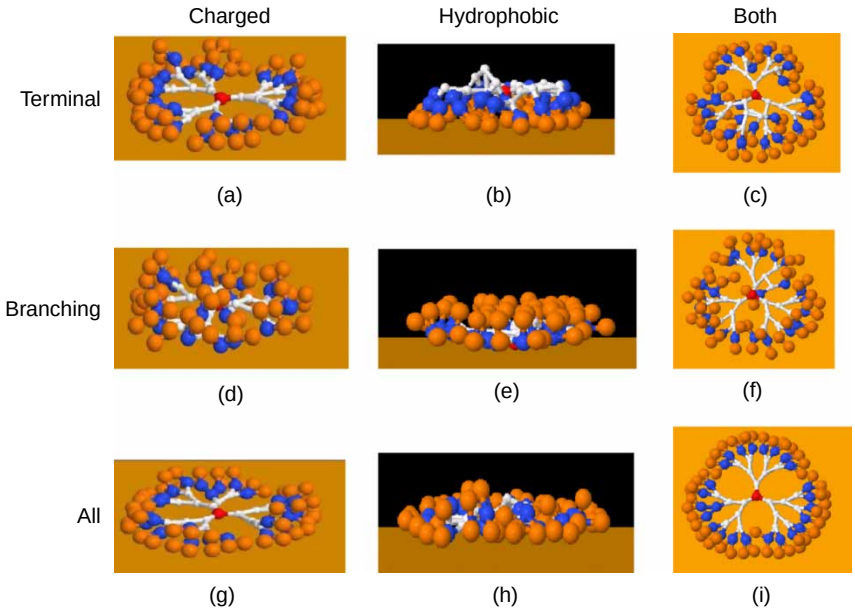

Figure 7. Conformations for a $G = 4$ adsorbed dendrimer having various charged/hydrophobic group distributions. The quantities $\kappa = 0.1$ and $A = 10$ are used for the adsorption of a charged dendrimer and a hydrophobic dendrimer, respectively. In the case of a charged and hydrophobic dendrimer, $\kappa = 0.1$ and $A = 5$ are used. The yellow surface is the adsorbing surface, gold beads are the terminal beads, blue beads are penultimate beads, a red bead is the core bead, and the remaining white beads are the other branching beads.

with (b), (d) with (e) and (g) with (h), we find that an adsorbed charged dendrimer expands whereas an adsorbed hydrophobic dendrimer forms a more compact structure. Similarly, we find that with charged dendrimers, most of the beads are on concentric circles with their centre being at the core bead. However, only a few beads of the adsorbed hydrophobic dendrimer are on concentric circles. We also find that with dendrimers having charged terminal groups or all charged groups, terminal beads are at the dendrimer periphery (Figure 7(a),(g)). In contrast, terminal beads are near the centre-of-mass for adsorbed hydrophobic dendrimers having all hydrophobic groups or hydrophobic terminal groups (Figure 7(b),(h), and also Figure 3(b)). It can also be seen that all beads are not attached to the surface when dendrimers are adsorbed due to electrostatic or hydrophobic interactions. Some of the beads are always in free solution. Using a charged dendrimer, not even all terminal beads can be attached to the surface (Figure 7(a),(g)). However, using a hydrophobic dendrimer, all terminal beads can be attached to the surface (Figures 7(b) and 5(b)).

We next investigate the effects of hydrophobicity on charged dendrimer adsorption. Looking at Figure 7(c),(f),(i), we find that the adsorbed charged and hydrophobic dendrimer also expands similar to adsorbed charged dendrimers. Comparing adsorbed charged dendrimers with adsorbed charged and hydrophobic dendrimers, we see that the effect of hydrophobicity on the dendrimer conformation is more pronounced on a terminally charged dendrimer than dendrimers having the other two charge distributions. The plausible reason could be that terminal groups are not connected each other, and thus two terminal beads can be placed nearby and move in the dendrimer volume, as seen in Figure 7(c). In the case of a dendrimer having charged branching beads, charged branching beads are connected to each other, making it difficult for them to come close together. Thus, we find that only a few branching beads come near the centre-of-mass (Figure 7(f)). In the case of a dendrimer having all charged beads, the effect of hydrophobicity on the dendrimer conformation is negligible since neither charged terminal groups nor branching beads can come near the centre-of-mass, making the dendrimer structure very similar to the charged dendrimer case (Figure 7(g),(i)).

As mentioned above and in the previous sections, adsorbed hydrophobic dendrimers have distinct conformations, which could not be achieved using a charged dendrimer. For example, we can preferentially place most of the terminal beads near surfaces using a dendrimer having hydrophobic terminal groups (cf. Figures 4(b) and 5(b)). Note that such dendrimer conformations cannot be achieved using electrostatic interactions. Thus, if the conformations obtained using hydrophobic dendrimers are suitable for desired applications, hydrophobic dendrimers should be used and may be synthesised [6–10]. We have also seen that a unique conformation can be achieved using a charged and hydrophobic dendrimer (Figure 7(c)), where most of terminal beads are attached to the surface and they are also at the dendrimer periphery, which is not possible either by a charged dendrimer or a hydrophobic

dendrimer. Thus, if such a conformation is required, then a charged and hydrophobic dendrimer can be used.

4. Summary and conclusions

We have investigated isolated hydrophobic dendrimer adsorption onto a flat surface using BD simulations. The dendrimer is described using a bead-rod model. Bead–bead and bead–surface hydrophobic interactions along with excluded-volume interactions have been modelled using a Lennard-Jones potential. Dendrimers having three different hydrophobic group distributions, i.e. only hydrophobic terminal beads, only hydrophobic branching beads, and all hydrophobic beads, have been considered. The effects of the strength of hydrophobicity, dendrimer generation and hydrophobicity distributions on the dendrimer conformation and monomer (bead) distributions within a dendrimer and near the surface are probed. Also, the effects of electrostatic interactions along with the hydrophobic interactions have been investigated.

Regardless of hydrophobic group distributions, adsorbed dendrimers adopt a disk-like conformation in which they flatten in the direction normal to the surface and expand in the direction parallel to the surface. As the strength of hydrophobicity decreases, the disk expands in the normal direction and contracts in the parallel direction. At sufficiently low strength of hydrophobicity, the dendrimer desorbs and adopts a sphere-like conformation.

Total bead density and terminal bead density profiles with respect to the dendrimer centre-of-mass are different for adsorbed dendrimers and those in free solution since we find pronounced effects of hydrophobic bead–bead attraction in the case of the adsorbed hydrophobic dendrimers. For adsorbed dendrimers, the terminal beads tend to be localised slightly away from the centre of mass of the dendrimer. Density profiles with respect to the surface show that the dendrimer forms a two-layer structure, with one layer corresponding to adsorbed beads and a second, less dense layer, corresponding to beads in free solution. Dendrimers having all hydrophobic groups have the largest number of beads in contact with the surface at fairly low strength of hydrophobicity, but this number decreases as the strength of hydrophobicity decreases. Similarly, a dendrimer having only hydrophobic branching groups and a dendrimer having only hydrophobic terminal groups have a comparable number of beads adsorbed to the surface, and this number also decreases as the dendrimer–surface attraction decreases. The terminal density profiles with respect to the surface reveal that nearly all terminal beads can be attached to the surface using a dendrimer having hydrophobic terminal beads or all hydrophobic beads. In the case of a dendrimer having hydrophobic branching beads, only a few terminal beads are attached to the surface and most of them are in free solution.

Comparing an adsorbed charged dendrimer with an adsorbed hydrophobic dendrimer reveals that the adsorbed hydrophobic dendrimer has a different conformation. For example, nearly all terminal beads can be attached to the surface using dendrimers having all hydrophobic beads or hydrophobic terminal beads, and terminal beads are localised slightly away from the centre of mass. These conformations are not possible with the charged dendrimer adsorption investigated in our previous study [22]. Considering a charged and hydrophobic dendrimer, we find that unique dendrimer conformations near the surface can be achieved, which are not likely to happen with a charge or hydrophobic interaction alone. For example, attaching nearly all terminal beads to the surface and placing them at the dendrimer periphery can only be achieved using a charged and hydrophobic dendrimer.

This study on hydrophobic dendrimer adsorption reveals a number of dendrimer conformations near surfaces which were not observed in our previous study of charged dendrimer adsorption. In addition, it has also investigated the competing effects of electrostatic and hydrophobic interactions, providing insight into how a dendrimer conformation can be controlled using a combination of charge and hydrophobic interactions. The present analysis may help guide dendrimer design for applications such as drug delivery and surface functionalisation, and provides a basis for future studies that use more complex models to probe the roles of counterions and dendrimer concentration.

Acknowledgements

We thank Dr Jan Andzelm, Dr Joshua Orlicki, and Dr Adam Rawlett of the Army Research Laboratory for helpful discussions. This material is based upon work supported in part by the US Army Research Laboratory and the US Army Research Office under Grant W911 NF-04-1-0265. Our work was also supported in part by the Army High Performance Computing Research Centre under the auspices of the Department of the Army, Army Research Laboratory (ARL) under Cooperative Agreement DAAD19-01-2-0014. The content does not necessarily reflect the position or policy of the government, and no official endorsement should be inferred. B.S. thanks the Graduate School of the University of Minnesota for financial support through the Doctoral Dissertation Fellowship program.

References

[1] C.C. Lee, J.A. MacKay, J.M.J. Frechet, and F.C. Szoka, *Designing dendrimers for biological applications*, Nat. Biotechnol. 23 (2005), pp. 1517–1526.
[2] A.K. Patri, I.J. Majoros, and J.R. Baker, Jr., *Dendritic polymer macromolecular carriers for drug delivery*, Curr. Opin. Chem. Biol. 6 (2002), pp. 466–471.
[3] V.J. Venditto, C.A. Regino, and M.W. Brechbiel, *PAMAM dendrimer based macromolecules as improved contrast agents*, Mol. Pharmacol. 2 (2005), pp. 302–311.
[4] A.M. Caminade, C. Padie, R. Laurent, A. Maraval, and J.P. Majoral, *Uses of dendrimers for DNA microarrays*, Sensors 6 (2006), pp. 901–914.

[5] D.C. Tully and J.M.J. Frechet, *Dendrimers at surfaces and interfaces: Chemistry and applications*, Chem. Commun. 14 (2001), pp. 1229–1239.

[6] R. Esfanda and D.A. Tomalia, *Poly(amidoamine) (PAMAM) dendrimers: From biomimicry to drug delivery and biomedical applications*, Drug Discov. Today 6 (2001), pp. 427–436.

[7] D.M. Watkins, Y. Sayed-Sweet, J.W. Klimash, N.J. Turro, and D.A. Tomalia, *Dendrimers with hydrophobic cores and the formation of supramolecular dendrimer-surfactant assemblies*, Langmuir 13 (1997), pp. 3136–3141.

[8] J.P. Kampf, C.W. Frank, E.E. Malmstrom, and C.J. Hawker, *Stability and molecular conformation of poly(benzyl ether) monodendrons with oligo(ethylene glycol) tails at the air–water interface*, Langmuir 15 (1999), pp. 227–233.

[9] A. Clouet, T. Darbre, and J.L. Reymond, *Esterolytic peptide dendrimers with a hydrophobic core and catalytic residues at the surface*, Adv. Synth. Catal. 346 (2004), pp. 1195–1204.

[10] M.R. Knecht, J.C. Garcia-Martinez, and R.M. Crooks, *Hydrophobic dendrimers as templates for Au nanoparticles*, Langmuir 21 (2005), pp. 11981–11986.

[11] A.K. Patri, J.F. Kukowska-Latallo, and J.R. Baker, Jr., *Targeted drug delivery with dendrimers: Comparison of the release kinetics of covalently conjugated drug and non-covalent drug inclusion complex*, Adv. Drug Deliv. Rev. 57 (2005), pp. 2203–2214.

[12] M. Ballauff and C.N. Likos, *Dendrimers in solution: Insight from theory and simulation*, Angew. Chem. Int. Ed. 43 (2004), pp. 2998–3020.

[13] V. Hierlemann, J.K. Campbell, L.A. Baker, R.M. Crooks, and A.J. Ricco, *Structure distortion of dendrimers on gold surfaces: A tapping-mode AFM investigation*, J. Am. Chem. Soc. 120 (1998), pp. 5323–5324.

[14] K.M.A. Rahman, C.J. Durning, N.J. Turro, and D.A. Tomilia, *Adsorption of poly(amidoamine) dendrimers on gold*, Langmuir 16 (2000), pp. 10154–10160.

[15] J.M. Kleijn, D. Barten, and M.A.C. Stuart, *Adsorption of charged macromolecules at a gold electrode*, Langmuir 20 (2004), pp. 9703–9713.

[16] V.V. Tsukruk, F. Rinderspacher, and V.N. Bliznyuk, *Self-assembled multilayer films from dendrimers*, Langmuir 16 (1997), pp. 2171–2176.

[17] R.C. van Duijvenbode, G.J.M. Koper, and M.R. Bohmer, *Adsorption of poly(propylene imine) dendrimers on glass. An interplay between surfaces and particle properties*, Langmuir 16 (2000), pp. 7713–7719.

[18] K. Esumi and M. Goino, *Adsorption of poly(amidoamine) dendrimers on alumina/water and silica/water interfaces*, Langmuir 14 (1998), pp. 4466–4470.

[19] A. Mecke, I. Lee, J.R. Baker, Jr., M.M.B. Holl, and B.G. Orr, *Deformability of poly(amidoamine) dendrimers*, Eur. Phys. J. E 14 (2004), pp. 7–16.

[20] Z. Pan, P. Somasundaran, N.J. Turro, and S. Jockusch, *Interactions of cataionic dendrimers with hematite mineral*, Colloid Surf. A 238 (2004), pp. 123–126.

[21] B.P. Cahill, G. Papastavrou, G.J.M. Koper, and M. Borkovec, *Adsorption of poly(amido amine) (PAMAM) dendrimers on silica: Importance of electrostatic three-body attraction*, Langmuir 24 (2008), pp. 465–473.

[22] B. Suman and S. Kumar, *Adsorption of charged dendrimers: A Brownian dynamics study*, J. Phys. Chem. B 111 (2007), pp. 8728–8739.

[23] M.L. Mansfield, *Surface adsorption of model dendrimers*, Polymer 37 (1996), pp. 3835–3841.

[24] A. Striolo and J.M. Prausnitz, *Adsorption of branched homopolymers on a solid surface*, J. Chem. Phys. 114 (2001), pp. 8565–8572.

[25] M. Ratner, I. Neelov, F. Sundholm, and B. Grinyov, *Brownian dynamics simulation of model dendrimer adsorption by an attractive surface*, Funct. Mater. 10 (2003), pp. 173–175.

[26] C. Pangali, M. Rao, and B.J. Berne, *A Monte Carlo simulation of the hydrophobic interaction*, J. Chem. Phys. 71 (1979), pp. 2975–2981.

[27] S. Brown, N.J. Fawzi, and T. Head-Gordon, *Coarse-grained sequences for protein folding and design*, Proc. Natl Acad. Sci. USA 100 (2003), pp. 10712–10717.

[28] M. Isobe, H. Shimizub, and Y. Hiwataric, *A multicanonical molecular dynamics study for a model protein-g*, Comput. Phys. Commun. 142 (2001), pp. 144–147.

[29] A.V. Lyulin, G.R. Davies, and D.B. Adolf, *Location of terminal groups of dendrimers: Brownian dynamics simulation*, Macromolecules 33 (2000), pp. 6899–6900.

[30] S.V. Lyulin, A.A. Darinskii, A.V. Lyulin, and M.A.J. Michels, *Computer simulation of dynamics of neutral and charged dendrimers*, Macromolecules 37 (2004), pp. 4676–4685.

[31] S.V. Lyulin, A.V. Lyulin, and A.A. Darinskii, *Brownian dynamics simulation of charged dendrimers: Statistical properties*, Polym. Sci. Ser. A 46 (2004), pp. 189–195.

[32] C.J. Oss, D.R. Absolom, and A. W. Neumann, *The hydrophobic effects: Essentially a van der Waals interaction*, Colloid Polym. Sci. 258 (1980), pp. 424–427.

[33] A. Rey, J.J. Freire, and J.G. de la Torre, *Monte Carlo calculations for linear chains and star polymers with intramolecular interactions. 3. Dimensions and hydrodynamic properties in good solvent conditions*, Macromolecules 20 (1987), pp. 2385–2390.

[34] I. Bitsanis and G. Hadziioannou, *Molecular dynamics simulations of the structure and dynamics of confined polymer melts*, J. Chem. Phys. 92 (1990), pp. 3827–3847.

[35] D.L. Ermak and J.A. McCammon, *Brownian dynamics with hydrodynamic interactions*, J. Chem. Phys. 69 (1978), pp. 1352–1360.

[36] J.P. Ryckaert, G. Ciccotti, and H.J.C. Berendsen, *Numerical integration of the cartesian equations of motion of a system with constraints: Molecular dynamics of n-alkanes*, J. Comput. Phys. 23 (1977), pp. 327–341.

[37] V. Krautler, W.F. van Gunsteren, and P.H. Hünenberger, *A fast SHAKE algorithm to solve distance constraint equations for small molecules in molecular dynamics simulations*, J. Comput. Chem. 5 (2001), pp. 501–508.

[38] J.N. Israelachvili, *Intermolecular and Surface Forces*, Academic Press, London, 1992.

[39] D.A. Tomalia, *Birth of a new macromolecular architecture: Dendrimers as quantized building blocks for nanoscale synthetic polymer chemistry*, Prog. Polym. Sci. 30(294) (2005), pp. 294–324.

[40] T.J. Prosa, B.J. Bauer, and E.J. Amis, *From stars to spheres: A SAXS analysis of dilute dendrimer solutions*, Macromolecules 34(4897) (2001), pp. 4897–4906.

[41] M.F. Ottaviani, F. Montalti, M. Romanelli, N.J. Turro, and D.A. Tomalia, *Characterization of starburst dendrimers by EPR. 4. Mn(II) as a probe of interphase properties*, J. Phys. Chem. 100(11033) (1996), pp. 11033–11042.

[42] D. Cakara, J. Kleimann, and M. Borkovec, *Microscopic protonation equilibria of poly(amidoamine) dendrimers from macroscopic titrations*, Macromolecules 36(4201) (2003), pp. 4201–4207.

[43] P.K. Maiti, T. Cagin, S.T. Lin, and W.A. Goddard, *Effect of solvent and pH on the structure of PAMAM dendrimers*, Macromolecules 38(979) (2005), pp. 979–991.

[44] M. Murat and G. Grest, *Molecular dynamics study of dendrimer molecules in solvents of varying quality*, Macromolecules 29 (1996), pp. 1278–1285.